

OPEN ACCESS

EDITED BY Lin Wang, Zhejiang University, China

REVIEWED BY Monika Colombo, Aarhus University, Denmark Wei Yan, Zhejiang University, China

*CORRESPONDENCE
Yi Liu

☑ liuyiwchscu@126.com

Rui Li ⊠ leerui@tsinghua.edu.cn Su Lui

☑ lusuwcums@tom.com Na Hu

[†]These authors have contributed equally to this work and share first authorship

[†]These authors have contributed equally to this work and share senior authorship

RECEIVED 14 July 2025 ACCEPTED 20 October 2025 PUBLISHED 05 November 2025

CITATION

Xia C, Fu M, Tian R, Ren Y, Xu X, Zhang J, Xia C, You C, Hu N, Lui S, Li R and Liu Y (2025) Dynamic evolution of postoperative hemodynamics in moyamoya angiopathy: a quantitative assessment of 4D Flow MRI and prognostic relevance. Front. Neurol. 16:1665883.

doi: 10.3389/fneur.2025.1665883

COPYRIGHT

© 2025 Xia, Fu, Tian, Ren, Xu, Zhang, Xia, You, Hu, Lui, Li and Liu. This is an open-access article distributed under the terms of the Creative Commons Attribution License (CC BY). The use, distribution or reproduction in other forums is permitted, provided the original author(s) and the copyright owner(s) are credited and that the original publication in this journal is cited, in accordance with accepted academic practice. No use, distribution or reproduction is permitted which does not comply with these terms.

Dynamic evolution of postoperative hemodynamics in moyamoya angiopathy: a quantitative assessment of 4D Flow MRI and prognostic relevance

Chao Xia^{1,2,3,4†}, Mingzhu Fu^{5†}, Rui Tian^{1†}, Yutao Ren^{1,6}, Xu Xu⁷, Jinge Zhang⁷, Chunchao Xia⁷, Chao You¹, Na Hu^{2,3,4,8}*, Su Lui^{2,3,4,8}*, Rui Li⁵* and Yi Liu¹*

¹Department of Neurosurgery, West China Hospital, Sichuan University, Chengdu, China, ²Department of Radiology, and Functional and Molecular Imaging Key Laboratory of Sichuan Province, West China Hospital, Sichuan University, Chengdu, China, ³Huaxi MR Research Center (HMRRC), West China Hospital, Sichuan University, Chengdu, China, ⁴Research Unit of Psychoradiology, Chinese Academy of Medical Sciences, Chengdu, China, ⁵Center for Biomedical Imaging Research, Department of Biomedical Engineering, Tsinghua University, Beijing, China, ⁶Department of Neurosurgery, The First Affiliated Hospital of Xi'an Jiaotong University, Xi'an, China, ⁷Department of Radiology, West China Hospital, Sichuan University, Chengdu, China, ⁸Sichuan Provincial Engineering Research Center of Intelligent Medical Imaging, West China Hospital, Sichuan University, Chengdu, China

Purpose: The hemodynamic mechanisms underlying revascularization efficacy in moyamoya angiopathy (MMA) and their prognostic implications remain incompletely characterized. This study leverages four-dimensional flow magnetic resonance imaging (4D Flow MRI) to investigate longitudinal hemodynamic changes at the carotid siphons of MMA patients undergoing revascularization, and to evaluate their association with surgical outcomes.

Methods: A prospective cohort of 35 consecutive MMA patients undergoing unilateral revascularization was enrolled at West China Hospital from July 2018 to January 2020. Using 4D Flow MRI, hemodynamic parameters, including mean/maximum flow, velocity, and wall shear stress, were quantified in the ipsilateral and contralateral carotid siphons at three timepoints: baseline, 1-week postoperative, and 1-year follow-up. Repeated-measures analysis of variance with Bonferroni correction was employed to compare longitudinal changes and correlate findings with 1-year clinical (excellent, good, and poor) and imaging (cerebral perfusion status and Matsushima collateralization grade) outcomes.

Results: Baseline and 1-week postoperative assessments revealed that only velocity within contralateral carotid siphon significantly increased (mean velocity: from 20.52 [15.34–28.78] cm/s to 23.70 [16.01–39.06] cm/s, p=0.026; maximum velocity: from 29.26 [19.68–38.39] cm/s to 33.22 [20.99–50.95] cm/s, p=0.001). However, both carotid siphons demonstrated significant reductions in mean and maximum flow (ipsilateral: mean flow from 1.92 [0.65–3.53] mL/s to 1.31 [0.58–2.87] mL/s, p=0.043, maximum flow from 2.61 [0.93–4.95] mL/s to 1.97 [0.89–3.90] mL/s, p=0.036; contralateral: mean flow from 2.87 [0.91–4.12] mL/s to 2.14 [0.81–3.78] mL/s, p=0.010) at 1-year follow-up. Lower contralateral siphon flow at follow-up correlated with "good" (but not "excellent") clinical outcomes. Reduced flow in both siphons was associated with improved cerebral perfusion and robust collateralization (Matsushima grades A/B), whereas no changes were observed in patients with poor collaterals (Matsushima grade C).

Conclusion: 4D Flow MRI reveals delayed, bilateral hemodynamic remodeling in MMA at 1-year post-revascularization. These changes correlate with clinical improvement, enhanced perfusion, and collateral development, underscoring the technique utility in monitoring long-term cerebrovascular adaptation.

KEYWORDS

moyamoya angiopathy, 4D Flow MRI, hemodynamics, revascularization, prognostic

1 Introduction

Moyamoya angiopathy (MMA) is a rare, chronic cerebrovascular disease, characterized by progressive stenosis or occlusion of the internal carotid arteries (ICAs) and compensatory collateral vessel formation, which is typically staged using conventional angiographybased systems (e.g., the Suzuki scale) to classify its severity (1, 2). The etiology of MMA remains poorly understood, but abnormal hemodynamics are considered to play a crucial role in its pathogenesis (3, 4). Studies have shown that wall shear stress (WSS) in the distal region of ICAs is relatively low in MMA patients, suggesting that reduced WSS may contribute to the arterial pathology. Computational fluid dynamics studies of MMA have further demonstrated altered flow patterns in ICAs and adjacent communicating arteries (5), although these findings have been inconsistent across studies (6). Surgical revascularization, involving anastomosis of extracranial arteries to cortical vessels or indirect bypass techniques, aims to restore cerebral perfusion. The primary goal of revascularization is to improve cerebral hemodynamics, a crucial outcome that is often assessed by the presence or absence of perfusion improvement on postoperative imaging studies. However, the hemodynamic mechanisms underlying its therapeutic effects is unclear (7, 8).

Conventional imaging techniques for assessing hemodynamics (e.g., digital subtraction angiography [DSA] and computed tomography [CT]) typically involve radiation exposure, invasiveness, or indirect blood flow measurements (7). While DSA excellently depicts vascular anatomy and staging, and CT perfusion can quantify perfusion improvement, they lack the ability to comprehensively visualize complex flow patterns. Four-dimensional flow magnetic resonance imaging (4D Flow MRI) offers a non-invasive, direct technique for quantifying hemodynamic parameters throughout the cardiac cycle (9). This technique has been used to study various cerebrovascular and neurodegenerative conditions (10–14), demonstrating correlations between 4D Flow MRI-derived hemodynamic biomarkers and clinical features or outcomes. However, 4D Flow MRI has not been systematically explored in MMA.

Given the potential of 4D Flow MRI to provide detailed hemodynamic information, we aimed to apply this technique to MMA patients. Specifically, the carotid siphons, critical segments adjacent to the stenotic/occluded part of the ICAs in MMA, exhibit unique physiological flow characteristics essential to understanding disease pathophysiology. Their unique S-shaped geometry inherently generates complex helical flow patterns and flow separation, which

Abbreviations: MMA, Moyamoya angiopathy; ICA, Internal carotid artery; WSS, Wall shear stress; MRI, Magnetic resonance imaging; DSA, digital subtraction angiography; CT, computed tomography; 4D Flow MRI, Four-dimensional flow magnetic resonance imaging.

predispose to pathologically low and oscillatory WSS (15, 16). These hemodynamic alterations create a vulnerable microenvironment that promotes endothelial dysfunction and atherosclerotic changes. In MMA, progressive morphological remodeling of the carotid siphons (e.g., luminal narrowing and tortuosity) further amplifies these disturbances, manifesting as elevated pressure drops and impaired cerebrovascular reserve (6, 7, 15, 17). Such hemodynamic parameters directly correlate with disease severity and clinical outcomes, providing mechanistic insights into why carotid siphon hemodynamics serve as critical biomarkers for assessing revascularization efficacy and long-term prognosis.

Therefore, we sought to investigate whether 4D Flow MRI could elucidate abnormal blood flow patterns through the carotid siphons. Furthermore, we aimed to determine whether the hemodynamic parameters measured by 4D Flow MRI are useful for assessing the outcomes of revascularization surgery.

2 Methods

2.1 Participants

This prospective observational study enrolled 35 patients with MMA from July 2018 to January 2020 at West China Hospital, Sichuan University. The study protocol was approved by the local institutional review board (No. 2018-219). Inclusion criteria were as follows: (1) diagnosis of moyamoya disease or moyamoya syndrome based on DSA according to established guidelines (18); (2) no prior revascularization; and (3) scheduled for unilateral revascularization surgery at the same hospital. Patients were required to undergo head imaging with 4D Flow MRI, CT perfusion, and DSA at three time points: before revascularization (baseline), 1 week after surgery, and 1 year after surgery (follow-up). Exclusion criteria included: (1) recent stroke (<3 months); (2) complete occlusion of bilateral carotid siphon based on DSA or 4D Flow MRI; (3) inadequate imaging quality; or (4) refusal of revascularization surgery. After enrollment, patients underwent unilateral combined revascularization surgery (details in Supplemental Materials). A power analysis based on our preliminary data from 20 patients indicated a minimum sample size of 26 to achieve 80% power ($\alpha = 0.05$) using G*Power software (version 3.1.9.6, German).

2.2 Head imaging

All MRI examinations were performed by experienced technologists (>5 years of MRI experience) using a 3.0-T Skyra scanner (Siemens Medical Systems, Erlangen, Germany) with a

20-channel head coil. Scout imaging was initially performed to estimate blood flow velocity in the carotid siphons and the circle of Willis. The following parameters were used during Scout acquisition: echo time, 3.4 ms; repetition time, 21 ms; slice thickness, 6 mm; flip angle, 20°; field of view read, 208 mm; field of view phase, 100.0%; resolution matrix, 272×275 ; baseline velocity encoding, 80-100 cm/s; and acquisition time, 65 s. Based on Scout measurements, an optimally personalized "velocity encoding" value was defined for each patient for 4D Flow MRI of the carotid siphons. MRI was performed using a free-breathing, peripheral pulse-gated, multi-shot turbo field echo sequence, with the following parameters: echo time, 2.7 ms; repetition time, 45 ms; slice thickness, 1 mm; slice gap, 0 mm; flip angle, 10° ; field of view read, 200 mm; field of view phase, 100.0%; resolution matrix, 256×216 ; and acquisition time, 19 min 50 s.

CT perfusion was performed using a 256-slice Revolution Apex scanner (GE Medical Systems, Brookfield, WI, USA) after injection of the contrast agent Iomeron® (Bracco, Milan, Italy) via a power injector at 4.5–5.0 mL/s. Imaging parameters were as follows: tube voltage, 80 kV; tube current, 300 mA; slice thickness, 5 mm; delay after injection of contrast agent, 5 s; cycle time, 2 s; number of slices, 640; and scan time, 50–55 s.

2.3 Analysis of 4D Flow MRI

Raw data from 4D Flow MRI were imported into VesselExplorer2 (V1.0.4.1, TSimaging Healthcare Co., Ltd., Beijing, China1). This software enables comprehensive analysis of 4D Flow MRI data, yielding key hemodynamic parameters and three-dimensionally dynamic visualization of blood flow patterns through streamline and pathline representations. Filtering thresholds were adjusted to maximize blood flow signal and minimize background noise. Velocity aliasing was minimized using anti-aliasing techniques. Following precise demarcation of carotid siphon segment boundaries, hemodynamic parameters (flow, velocity, and WSS) systematically quantified within cross-sectional planes at the posterior siphon bend, with both mean and maximum values recorded for comprehensive hemodynamic profiling. WSS, which accounts for both circumferential and axial components, reflects the tangential force exerted on vascular endothelial cells by blood flow (19). All blood flow measurements were independently performed by an experienced neuroradiologist (CX) and an experienced neurosurgeon (YTR). Discrepancies were resolved through consultation with a senior neuroradiologist (SL).

2.4 Assessment of revascularization outcomes at follow-up

Clinical outcomes were evaluated through standardized preoperative and postoperative assessments conducted by experienced neurologists. At 1-year follow-up, clinical outcomes were evaluated using a three-tiered classification system: (1) "excellent" indicated

complete resolution of preoperative neurological symptoms/signs (including dizziness, headache, limb weakness, memory impairment, and so on); (2) "good" referred to partial improvement with persistent but attenuated symptoms or signs; and (3) "poor" denoted unchanged or aggravated clinical manifestations compared to preoperative status. This evaluation combined patient self-reported symptom diaries with clinical examination findings, per established protocols referenced in prior literature (20). To ensure consistency, all assessments were performed blinded to imaging results, with discrepancies resolved through consensus discussions involving senior clinicians. This approach balances patient-centered outcomes with clinical objectivity while maintaining methodological rigor.

Imaging outcomes at 1-year follow-up were assessed independently by two experienced neuroradiologists (CX and MZF) under blinded conditions regarding clinical information. Discrepancies were resolved through consultation rounds with a senior neuroradiologist (SL). Cerebral perfusion was analyzed through serial CT perfusion scans (baseline vs. follow-up), quantified using the preinfarction staging system (21), with lower preinfarction stages reflecting improved perfusion. Collateral circulation was assessed by DSA and graded as A, B, or C using the Matsushima scale (Supplementary Figure S1) (22).

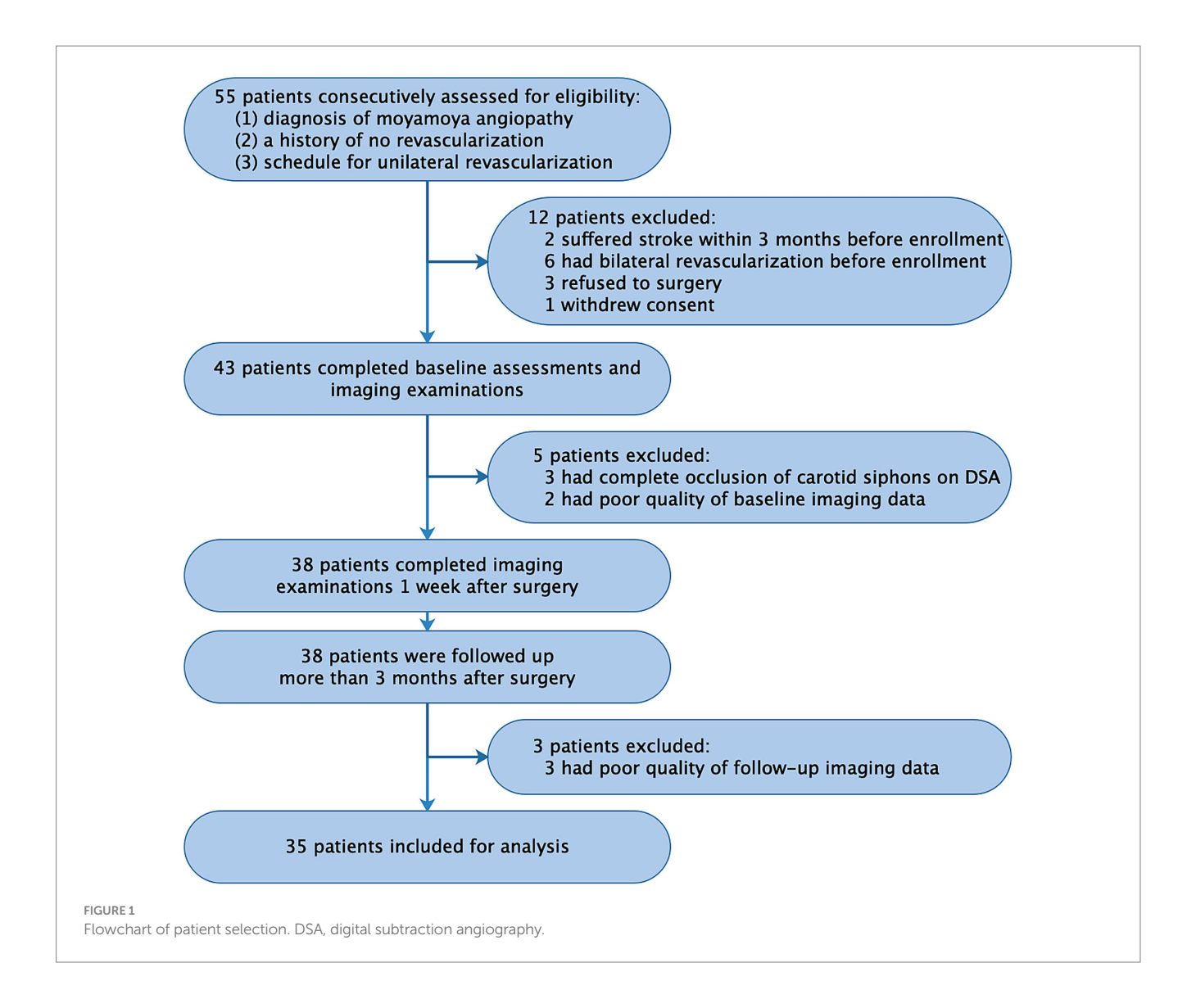
2.5 Statistical analysis

Data were statistically analyzed using SPSS 26.0 (IBM, Armonk, NY, USA), with results considered significant if associated with two-sided p < 0.05. Shapiro–Wilk test was performed before applying repeated-measures analysis of variance. Hemodynamic parameters in the ipsi- and contralateral carotid siphons were compared across three time points using repeated-measures analysis of variance for normally distributed data or Friedman test for non-normally distributed data, with Bonferroni corrections for multiple comparisons. Mauchly's tests of sphericity were conducted to check assumptions. Parameters were also analyzed in subgroups defined by sex, age category (< or ≥18 years), or disease stage (categorized as "early" if in Suzuki stages I-II, "intermediate" if in Suzuki stages III-IV, or "advanced" if in Suzuki stages V-VI) (18, 23, 24). Associations of hemodynamic parameters with clinicodemographic characteristics or outcomes at follow-up were explored using repeated-measures analysis of variance with Bonferroni correction for multiple comparisons. The interclass correlation coefficient was evaluate interobserver consistency to of blood flow measurements.

3 Results

We analyzed 35 patients (15 males; mean age, 34.3 ± 17.7 years; range, 6–69 years), including 10 pediatric patients (<18 years) (Figure 1 and Table 1). All patients underwent unilateral revascularization and completed 1-year postoperative follow-up. At follow-up, 19 patients (54.3%) achieved "excellent" clinical outcomes (complete resolution of preoperative symptoms), while 16 (45.7%) were classified as "good" (persistent but attenuated symptoms) (Table 2). A representative case was shown in Figure 2.

¹ http://www.tsimaging.net



3.1 Hemodynamic parameters via 4D Flow MRI

Baseline and 1-week postoperative assessments revealed that only velocity within contralateral carotid siphon significantly increased (mean: from 20.52 [15.34-28.78] cm/s to 23.70 [16.01-39.06] cm/s, p = 0.026; maximum: from 29.26 [19.68–38.39] cm/s to 33.22 [20.99– 50.95] cm/s, p = 0.001) (Figure 3 and Supplementary Table S1). However, significant reductions were observed between baseline and 1 year postoperatively: (1) Ipsilateral siphon: Mean flow decreased from 1.92 (0.65-3.53) mL/s to 1.31 (0.58-2.87) mL/s (p = 0.043), and maximum flow decreased from 2.61 (0.93-4.95) mL/s to 1.97 (0.89-3.90) mL/s (p = 0.036); and (2) Contralateral siphon: Mean flow decreased from 2.87 (0.91-4.12) mL/s to 2.14 (0.81-3.78) mL/s (p = 0.010). Additionally, significant reductions were found between 1 week and 1 year postoperatively: (1) Ipsilateral siphon: Maximum flow decreased from 2.58 (0.93-4.83) mL/s to 1.97 (0.89-3.90) mL/s (p = 0.036); and (2) Contralateral siphon: Mean flow decreased from 3.29 (0.99-4.34) mL/s to 2.14 (0.81-3.78) mL/s (p = 0.001), and maximum flow decreased from 4.36 (1.40-5.80) mL/s to 3.06 (0.96-5.14) mL/s (p=0.018). Interobserver reproducibility was excellent for flow measurements (interclass correlation coefficient > 0.83).

3.2 Subgroup analyses

Hemodynamic responses varied by sex, age, and disease stage. Females exhibited reductions in contralateral mean/maximum flow from 1 week to 1 year postoperatively (mean: from 3.25 [1.11–4.02] mL/s to 2.12 [0.65–3.20] mL/s, p=0.008; maximum: from 4.18 [1.44–5.45] mL/s to 2.89 [0.97–4.51] mL/s, p=0.013) and increases in contralateral maximum velocity from baseline to 1 week postoperatively (from 29.18 [18.28–29.23] cm/s to 31.55 [20.83–49.18] cm/s, p=0.013). However, no significant changes were observed in males (Supplementary Table S2). Adults (>18 years) demonstrated significant reductions in bilateral mean flow (surgical side: from 1.89 [0.86–4.06] mL/s to 1.48 [0.90–2.92] mL/s, p=0.049; contralateral side: from 3.59 [1.00–4.50] mL/s to 3.07 [1.32–3.85] mL/s, p=0.006), ipsilateral maximum flow (from 2.82 [1.30–5.65]

TABLE 1 Clinicodemographic characteristics of the 35 participants at baseline.

Characteristics	Patients (<i>n</i> = 35)
Age, yr	34.3 ± 17.7
Female	20 (57.1)
Hypertension	9 (25.7)
Diabetes mellitus	1 (2.9)
Current smoker	5 (14.3)
Current drinker	2 (5.7)
Presentation of moyamoya angiopathy	
Ischemic	30 (85.7)
Hemorrhagic	5 (14.3)
Suzuki stage, surgical/contralateral side	
Early	5 (14.3)/12 (34.3)
Intermediate	19 (54.3)/16 (45.7)
Advanced	11 (31.4)/7 (20.0)
Preinfarction stage, surgical/contralateral side	
0	0 (0)/1 (2.9)
I	10 (28.6)/20 (57.1)
П	10 (28.6)/2 (5.7)
III	3 (8.6)/1 (2.9)
IV	12 (34.3)/11 (31.4)

Values are n (%) or mean \pm SD.

TABLE 2 Outcomes of the 35 participants at 1-year follow-up.

Outcomes	Patients (<i>n</i> = 35)
Clinical condition	
Excellent	19 (54.3)
Good	16 (45.7)
Poor	0 (0)
Cerebral perfusion	
Better than at baseline	23 (65.7)
Not better than at baseline	12 (34.3)
Matsushima grade of collateralization	
A	12 (34.3)
В	13 (37.1)
С	10 (28.6)

Values are n (%).

mL/s to 2.07 [1.33–4.04] mL/s, p=0.033), and ipsilateral mean velocity (from 22.20 [15.07–30.21] cm/s to 16.19 [10.72–23.75] cm/s, p=0.006), whereas pediatric patients showed no significant changes (Supplementary Table S3). For early-stage disease (Suzuki I-II), significant reductions were observed in mean/maximum ipsilateral flow (mean: from 4.40 [3.75–4.90] mL/s to 3.80 [2.89–4.12] mL/s, p=0.034; maximum: from 5.95 [5.22–6.95] mL/s to 5.34 [3.67–5.90] mL/s, p=0.034); for intermediate-stage disease (Suzuki III-IV), significant decreases in ipsilateral maximum flow (from 2.87 [2.08–4.83] mL/s to 2.38 [1.72–3.90] mL/s, p=0.045), ipsilateral mean/maximum velocity (mean: from 22.20 [20.30–25.02] cm/s to 16.64

[11.20–22.61] cm/s, p = 0.006; maximum: from 30.45 [26.23–34.54] cm/s to 24.78 [15.55–30.54] cm/s, p = 0.028), and contralateral mean flow (from 3.10 [1.17–3.65] mL/s to 2.05 [1.25–3.20] mL/s, p = 0.014); and for advanced-stage disease (Suzuki V-VI), no hemodynamic changes detected (Supplementary Table S4–S6).

3.3 Surgical outcomes

Hemodynamic improvements correlated with clinical and imaging outcomes. Ipsilateral mean/maximum flow decreased significantly in both "excellent" and "good" outcome groups, while contralateral mean/maximum flow reductions were exclusive to the "good" outcome group (Figure 4 and Supplementary Table S7). Among 23 patients with improved preinfarction staging, ipsilateral flow/velocity decreased significantly; no changes were observed in the 12 patients without perfusion improvement (Figure 5 and Supplementary Table S8). Patients with robust collateralization (Matsushima grades A/B; n = 25) exhibited bilateral flow reductions, whereas those with poor collaterals (grade C; n = 10) showed no changes in flow or velocity (Figure 6 and Supplementary Table S9).

4 Discussion

Our study demonstrates that unilateral revascularization induces progressive, bilateral hemodynamic adaptation in MMA, with significant reductions in mean and maximum flow observed in both ipsi- and contralateral carotid siphons at 1-year follow-up. These changes were absent at 1 week postoperatively, suggesting delayed cerebrovascular remodeling rather than immediate flow redistribution. The association between reduced flow parameters and improved clinical outcomes, cerebral perfusion, and collateralization underscores the therapeutic relevance of these hemodynamic shifts. Notably, 4D Flow MRI enabled visualization of bilateral flow dynamics, offering mechanistic insights into revascularization efficacy and supporting its integration into postoperative surveillance protocols.

Our observation of diminished flow characteristics within the bilateral carotid siphons provides compelling experimental validation for computational fluid dynamic simulations that previously predicted analogous hemodynamic patterns in these vascular segments (25). The bilateral hemodynamic effects of unilateral revascularization likely reflect interconnected cerebrovascular adaptations. The circle of Willis and external carotid collateral networks, particularly the superficial temporal arteries, may mediate contralateral flow modulation, as hypothesized in computational models (25, 26). The persistent flow asymmetry (higher contralateral flow) at follow-up aligns with Suzuki stage-dependent stenosis severity where advanced ipsilateral occlusion necessitates complete perfusion shift to external carotid sources (15, 27). This compensatory mechanism may explain the lack of hemodynamic response in advanced-stage patients, as their cerebral circulation is already maximally redirected.

Subgroup analyses revealed critical age- and sex-related differences. Postmenopausal estrogen decline in females may reduce vascular adaptability, necessitating greater contralateral compensation (28). Conversely, children's robust intrinsic collateral capacity likely delays postoperative hemodynamic adaptation (29), while adults derive clearer benefit from revascularization-induced

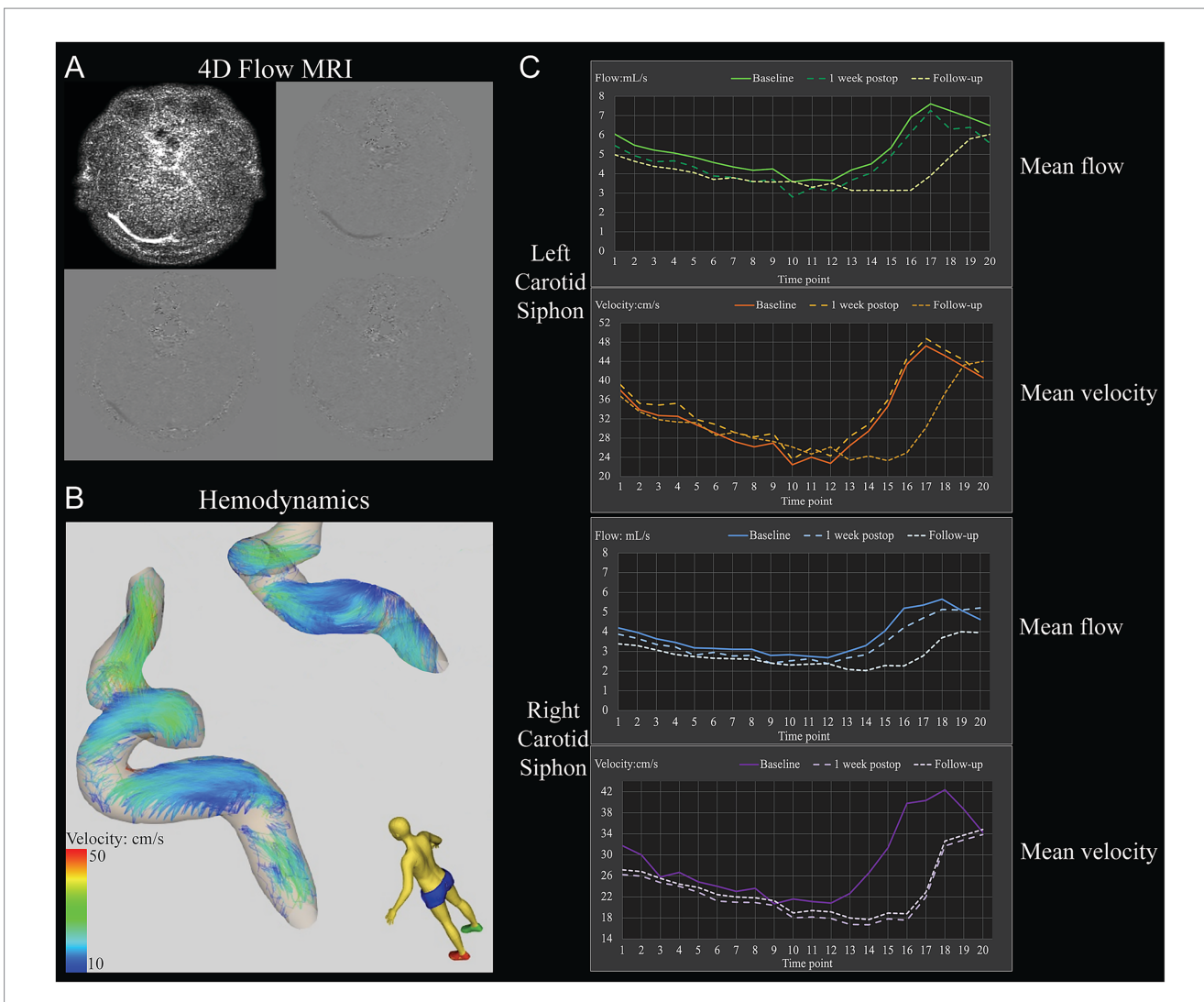


FIGURE 2

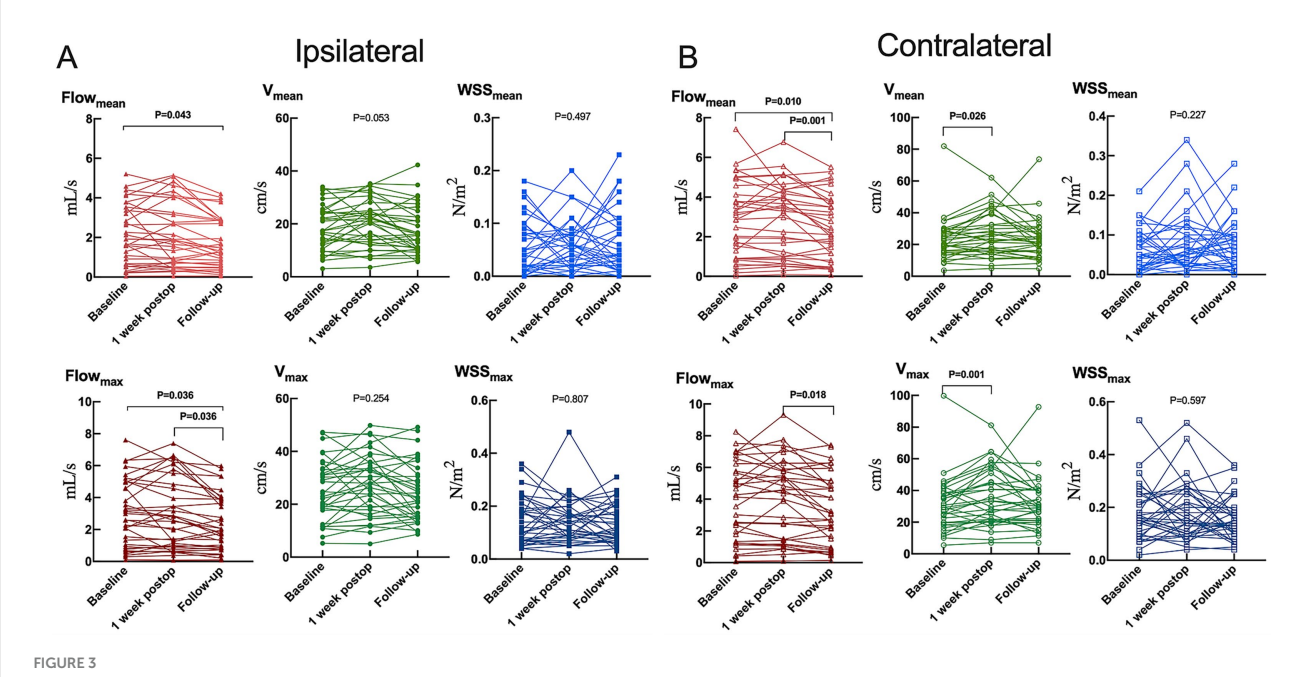
Example of the determination of hemodynamic parameters in the carotid siphons of a 31-year-old woman with moyamoya angiopathy who underwent left-side revascularization. (A) Raw 4D Flow MRI. (B) Pathline visualization of the bilateral carotid siphons. (C) Hemodynamic parameters included mean flow and mean velocity through the bilateral carotid siphons at different time points within one cardiac cycle before revascularization (baseline), 1 week after surgery, or 1 year after surgery (follow-up).

external carotid augmentation. These findings suggest that surgical timing and laterality should be individualized based on age, sex, and disease stage. Our analysis reveals a significant correlation between reduced mean and maximum flow in both ipsi- and contralateral carotid siphons and concurrent improvements in clinical status, cerebral perfusion, and adaptive intracranial vascular remodeling. Prior investigations with limited cohort sizes have identified associations between revascularization outcomes and alternate hemodynamic indicators, such as pressure gradients or posterior communicating artery flow dynamics (6, 8, 30). However, these findings primarily focused on isolated parameters. Future multicenter studies with larger patient populations should employ comprehensive hemodynamic profiling to elucidate the complete spectrum of vascular response metrics that most robustly characterize cerebrovascular reactivity surgical revascularization efficacy.

The stability of WSS parameters observed in our cohort aligns with findings from a cross-sectional analysis that similarly

reported no significant associations between WSS and incident cerebrovascular events (31). This discrepancy with another studies demonstrating links between low WSS with ICA stenosis (5, 7) may reflect methodological heterogeneities in outcome measurement or inherent differences in hemodynamic stressors between vascular beds. Compensatory vascular remodeling, including reduced carotid siphon tortuosity (32, 33), may stabilize endothelial shear stress, thereby mitigating maladaptive responses like inflammation or platelet aggregation (8, 34–36). This hypothesis warrants investigation through longitudinal histological correlation studies.

Our findings must be interpreted with caution given several methodological limitations. First, the observational study design and relatively small sample size inherently limit statistical generalizability. This necessitates replication in larger prospective cohorts with longitudinal follow-up. Despite these limitations, the heterogeneity of our sample allowed us to demonstrate differential relationships between hemodynamic parameters and outcomes in different patient



Hemodynamic parameters in the (A) ipsilateral or (B) contralateral carotid siphon before unilateral revascularization (baseline), at 1 week after surgery, or 1 year after surgery (follow-up). Flow_{mean}, mean flow; Flow_{max}, maximum flow; V_{mean} , mean velocity; V_{max} , maximum velocity; W_{mean} , mean wall shear stress on vascular endothelium; W_{max} maximum wall shear stress on vascular endothelium. Results are plotted individually for the 35 patients in the study.

subgroups. Second, 4D Flow MRI's limited spatial resolution (e.g., inability to assess vessels <1 mm) and potential motion artifacts may have influenced hemodynamic measurement. Nevertheless, our results substantiate the prognostic utility of this imaging modality in cerebrovascular disease characterization, underscoring the clinical imperative to advance technical development priorities. To fully realize its diagnostic potential in multicenter clinical trials, future research must emphasize the development of enhanced spatial resolution, accelerated acquisition protocols, and automated postprocessing pipelines (37). While the VesselExplorer2 software lacks direct pressure computation capabilities, our approach aligns with fluid dynamics principles: future studies will integrate the acquired velocity fields and flow rates into the Navier-Stokes equations to computationally derive pressure distributions. Such integration would advance mechanistic understanding of how flow alterations translate into vascular stress and surgical outcome predictors, bridging a key gap in current MMA hemodynamic assessment paradigms.

5 Conclusion

This study establishes 4D Flow MRI as a powerful tool for monitoring long-term hemodynamic changes after MMA revascularization. The bilateral flow reductions observed at 1 year correlate with improved clinical and perfusion outcomes, supporting the technique's use in evaluating surgical efficacy and guiding personalized management strategies. While WSS stability requires further investigation, our findings collectively advocate for integrating advanced hemodynamic imaging into MMA care pathways to optimize therapeutic decision-making.

Data availability statement

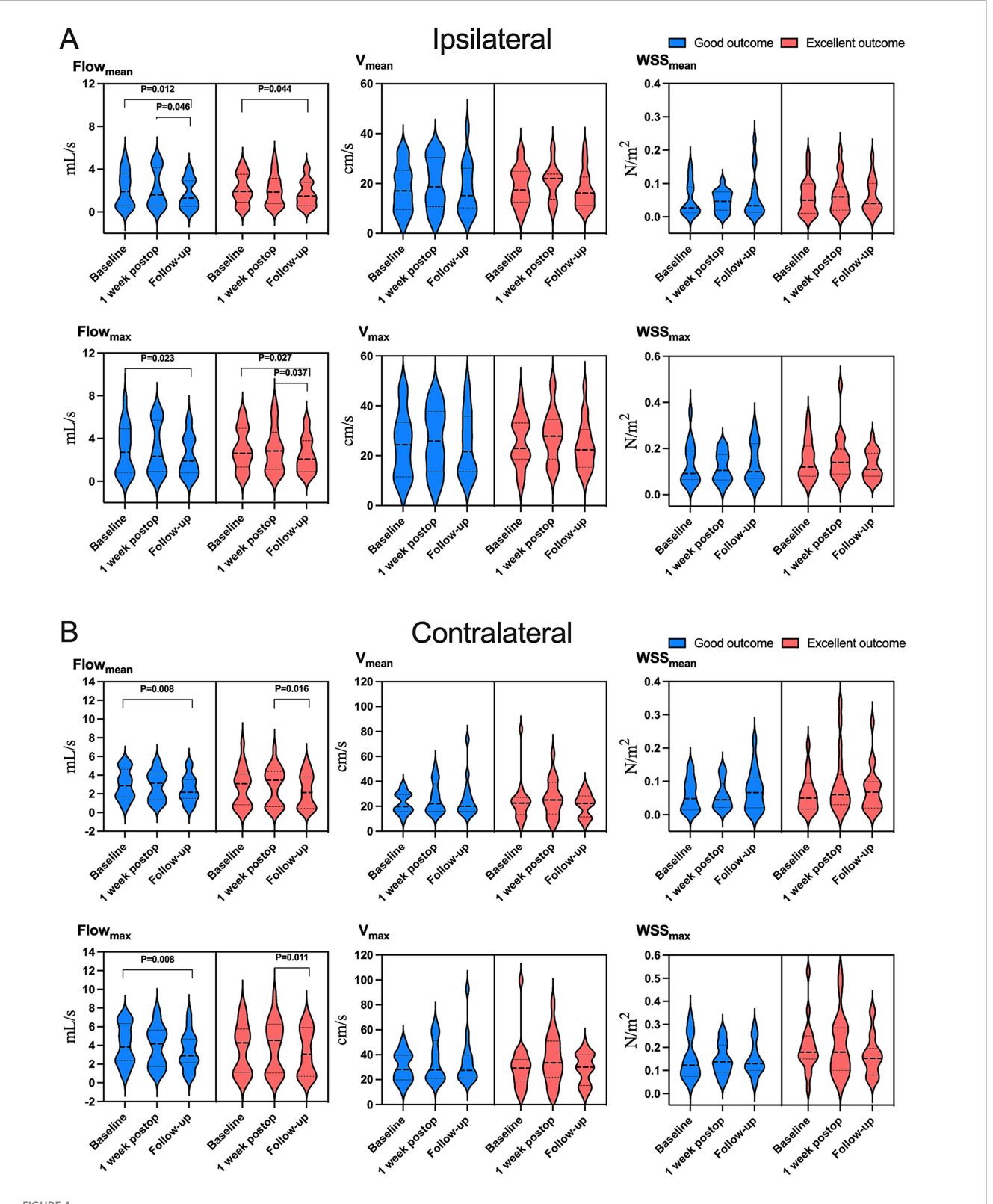
The raw data supporting the conclusions of this article will be made available by the authors, without undue reservation.

Ethics statement

The studies involving humans were approved by the Ethics Committee on Biomedical Research of West China Hospital, Sichuan University (Approval number: 2018-219). The studies were conducted in accordance with the local legislation and institutional requirements. Written informed consent for participation in this study was provided by the participants or their legal guardians.

Author contributions

CX: Conceptualization, Data curation, Formal analysis, Funding acquisition, Investigation, Methodology, Validation, Visualization, Writing – original draft, Writing – review & editing. MF: Data curation, Formal analysis, Investigation, Methodology, Resources, Software, Validation, Visualization, Writing – review & editing. RT: Conceptualization, Data curation, Methodology, Software, Supervision, Validation, Visualization, Writing – review & editing. YR: Data curation, Formal analysis, Investigation, Methodology, Resources, Validation, Visualization, Writing – review & editing. XX: Data curation, Formal analysis, Investigation, Validation, Visualization, Writing – review & editing. JZ: Data curation, Formal analysis, Investigation, Validation, Visualization, Writing – review & editing. CCX: Formal analysis, Investigation, Methodology, Supervision, Validation, Writing – review &



Variation in hemodynamic parameters in **(A)** ipsilateral or **(B)** contralateral carotid siphons in subsets of patients who were in "excellent" clinical condition (red) or "good" condition (blue) at follow-up (see Methods). Flow_{mean}, mean flow; Flow_{max}, maximum flow; V_{mean}, mean velocity; V_{max}, maximum velocity; WSS_{mean}, mean wall shear stress on vascular endothelium; WSS_{max}, maximum wall shear stress on vascular endothelium.

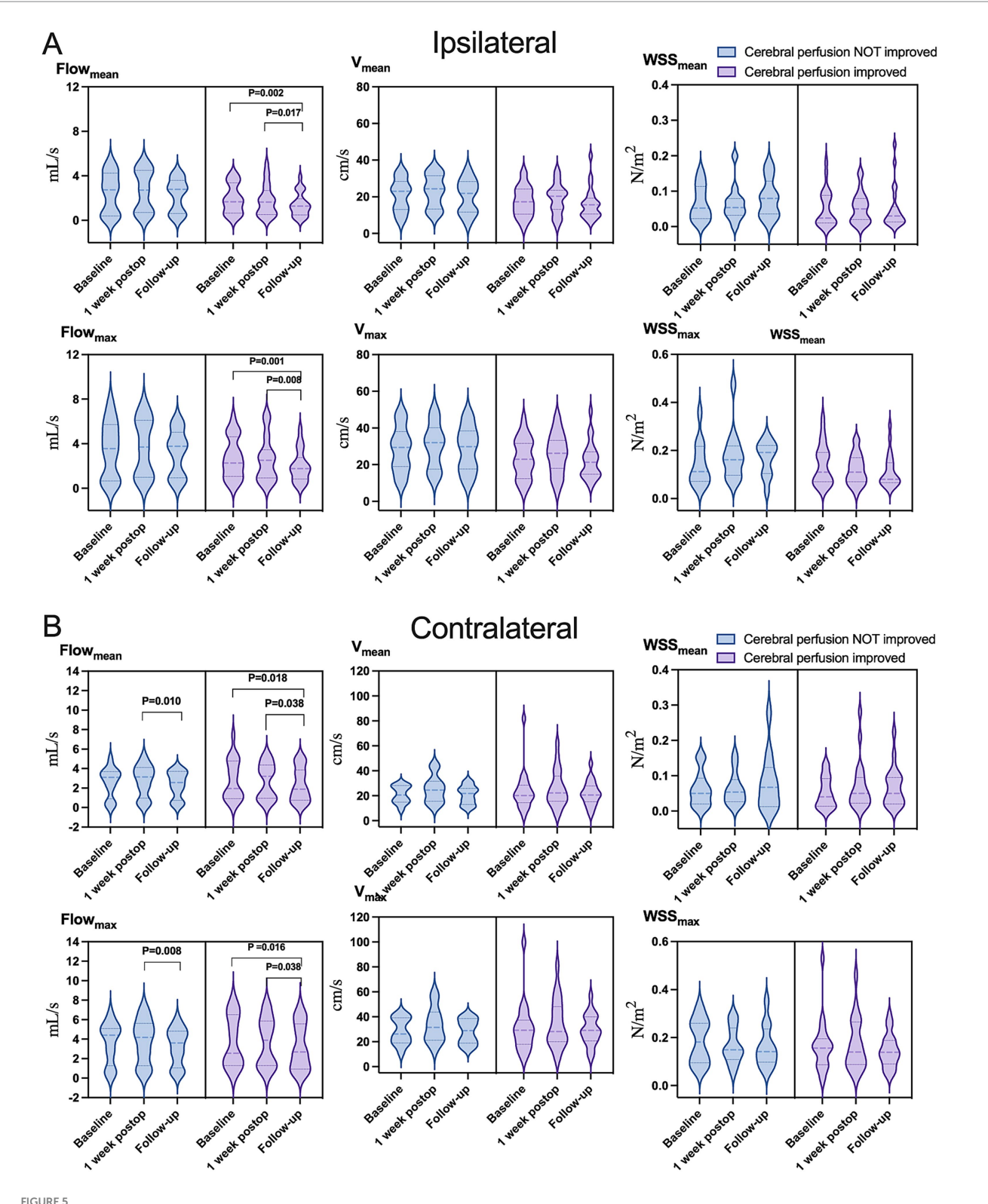
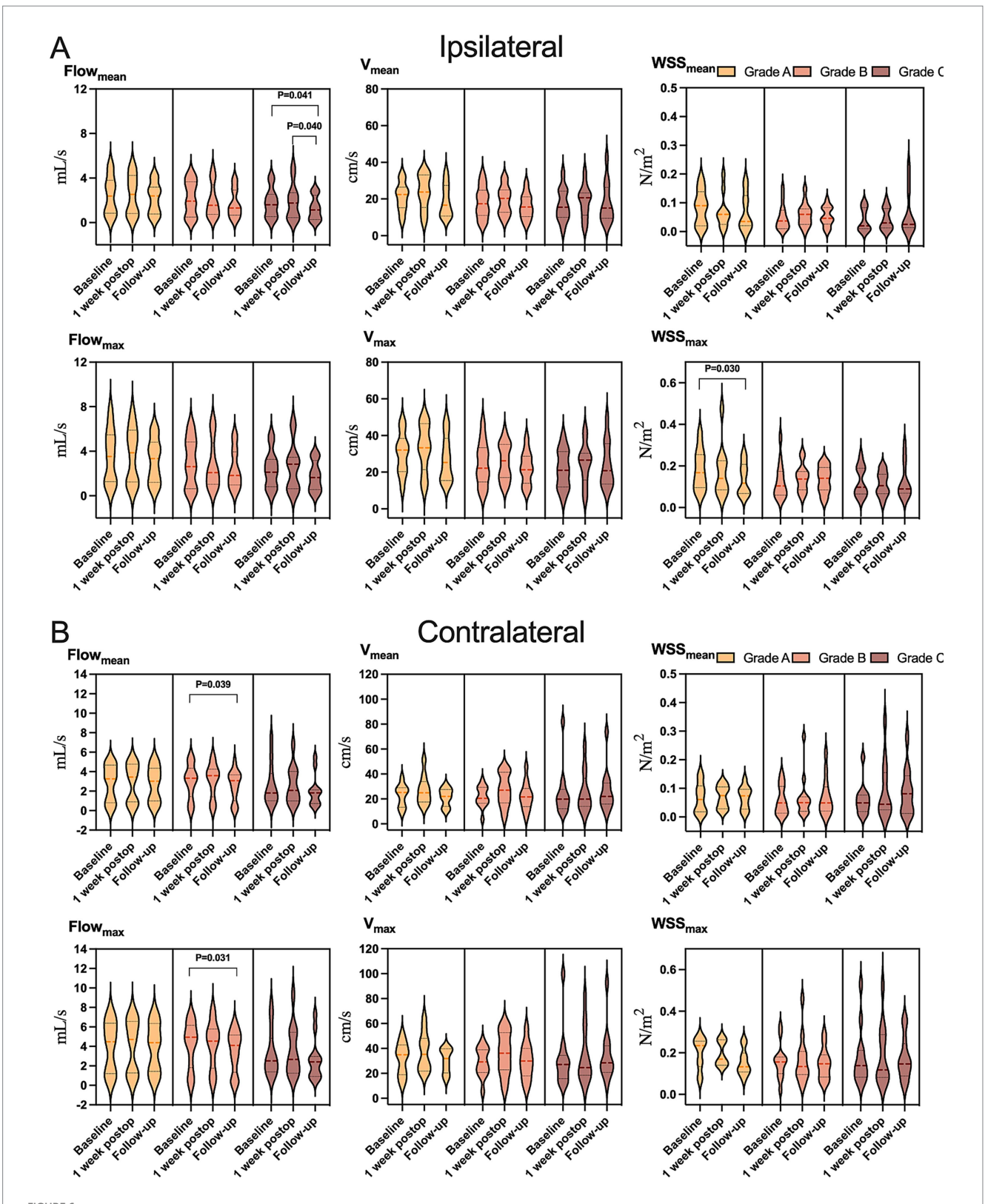


FIGURE 5 Variation in hemodynamic parameters in (A) ipsilateral or (B) contralateral carotid siphons in subsets of patients who showed improved cerebral perfusion (light purple) or not (light blue) at follow-up. Flow_{mean}, mean flow; Flow_{mean}, mean flow; V_{mean}, mean velocity; V_{mean}, mean velocity; V_{mean}, mean wall shear stress on vascular endothelium; WSS_{max}, maximum wall shear stress on vascular endothelium.



Variation in hemodynamic parameters in **(A)** ipsilateral or **(B)** contralateral carotid siphons in subsets of patients who showed postoperative collateralization of grade A (light yellow), grade B (yellow), or grade C (dark yellow) at follow-up. Flow_{mean}, mean flow; Flow_{max}, maximum flow; V_{mean}, mean velocity; V_{max}, maximum velocity; WSS_{mean}, mean wall shear stress on vascular endothelium; WSS_{max}, maximum wall shear stress on vascular endothelium.

editing. CY: Conceptualization, Data curation, Investigation, Methodology, Project administration, Resources, Supervision, Writing – review & editing. NH: Conceptualization, Data curation, Funding acquisition, Investigation, Methodology, Project administration, Resources, Supervision, Validation, Visualization, Writing – review & editing. SL: Conceptualization, Funding acquisition, Investigation, Methodology, Project administration, Resources, Supervision, Visualization, Writing – review & editing. RL: Data curation, Investigation, Methodology, Resources, Software, Visualization, Writing – review & editing. YL: Conceptualization, Data curation, Investigation, Methodology, Project administration, Resources, Supervision, Validation, Visualization, Writing – review & editing.

Funding

The author(s) declare that financial support was received for the research and/or publication of this article. This study was supported by grants from the Noncommunicable Chronic Diseases-National Science and Technology Major Project (2024ZD0527700/2024ZD0527704), National Natural Science Foundation of China (82441007, 82120108014), Key R&D Project of Chengdu Science and Technology Office (2024-YF05-00443-SN), 1-3-5 Project for Disciplines of Excellence (ZYGD23003) and Artificial Intelligence (ZYAI24010), West China Hospital, Sichuan University, and Sichuan University Postdoctoral Interdisciplinary Innovation Fund (JCXK2209).

Acknowledgments

The authors thank the patients for participating in this study.

References

- 1. Suzuki J, Takaku A. Cerebrovascular "moyamoya" disease. Disease showing abnormal net-like vessels in base of brain. *Arch Neurol.* (1969) 20:288–99. doi: 10.1001/archneur.1969.00480090076012
- 2. Kuroda S, Houkin K. Moyamoya disease: current concepts and future perspectives. Lancet Neurol. (2008) 7:1056–66. doi: 10.1016/s1474-4422(08)70240-0
- 3. Uehara T, Bang OY, Kim JS, Minematsu K, Sacco R. Risk factors. Front Neurol Neurosci. (2016) 40:47–57. doi: 10.1159/000448301
- 4. Lee M, Zaharchuk G, Guzman R, Achrol A, Bell-Stephens T, Steinberg GK. Quantitative hemodynamic studies in moyamoya disease: a review. *Neurosurg Focus*. (2009) 26:E5. doi: 10.3171/2009.1.Focus08300
- 5. Seol HJ, Shin DC, Kim YS, Shim EB, Kim SK, Cho BK, et al. Computational analysis of hemodynamics using a two-dimensional model in moyamoya disease. *J Neurosurg Pediatr*. (2010) 5:297–301. doi: 10.3171/2009.10.Peds09452
- 6. Sun W, Ruan Z, Dai X, Li S, Li S, Zhang J, et al. Quantifying hemodynamic changes in moyamoya disease based on two-dimensional cine phase-contrast magnetic resonance imaging and computational fluid dynamics. *World Neurosurg.* (2018) 120:e1301–9. doi: 10.1016/j.wneu.2018.09.057
- 7. Jamil M, Tan GX, Huq M, Kang H, Lee ZR, Tang PH, et al. Changes to the geometry and fluid mechanics of the carotid siphon in the pediatric moyamoya disease. *Comput Methods Biomech Biomed Engin.* (2016) 19:1760–71. doi:10.1080/10255842.2016.1184655
- 8. Zhu F, Karunanithi K, Qian Y, Mao Y, Xu B, Gu Y, et al. Assessing surgical treatment outcome following superficial temporal artery to middle cerebral artery bypass based on computational haemodynamic analysis. *J Biomech.* (2015) 48:4053–8. doi: 10.1016/j.jbiomech.2015.10.005
- 9. Soulat G, McCarthy P, Markl M. 4D flow with MRI. Annu Rev Biomed Eng. (2020) 22:103–26. doi: 10.1146/annurev-bioeng-100219-110055
- 10. Rivera-Rivera LA, Cody KA, Eisenmenger L, Cary P, Rowley HA, Carlsson CM, et al. Assessment of vascular stiffness in the internal carotid artery proximal to the

Conflict of interest

The authors declare that the research was conducted in the absence of any commercial or financial relationships that could be construed as a potential conflict of interest.

Generative AI statement

The authors declare that no Gen AI was used in the creation of this manuscript.

Any alternative text (alt text) provided alongside figures in this article has been generated by Frontiers with the support of artificial intelligence and reasonable efforts have been made to ensure accuracy, including review by the authors wherever possible. If you identify any issues, please contact us.

Publisher's note

All claims expressed in this article are solely those of the authors and do not necessarily represent those of their affiliated organizations, or those of the publisher, the editors and the reviewers. Any product that may be evaluated in this article, or claim that may be made by its manufacturer, is not guaranteed or endorsed by the publisher.

Supplementary material

The Supplementary material for this article can be found online at: https://www.frontiersin.org/articles/10.3389/fneur.2025.1665883/full#supplementary-material

- carotid canal in Alzheimer's disease using pulse wave velocity from low rank reconstructed 4D flow MRI. *J Cereb Blood Flow Metab.* (2021) 41:298–311. doi: 10.1177/0271678x20910302
- 11. Perera R, Isoda H, Ishiguro K, Mizuno T, Takehara Y, Terada M, et al. Assessing the risk of intracranial aneurysm rupture using morphological and hemodynamic biomarkers evaluated from magnetic resonance fluid dynamics and computational fluid dynamics. *Magn Reson Med Sci.* (2020) 19:333–44. doi: 10.2463/mrms.mp.2019-0107
- 12. Birnefeld J, Wåhlin A, Eklund A, Malm J. Cerebral arterial pulsatility is associated with features of small vessel disease in patients with acute stroke and TIA: a 4D flow MRI study. J Neurol. (2020) 267:721–30. doi: 10.1007/s00415-019-09620-6
- 13. Schuchardt F, Hennemuth A, Schroeder L, Meckel S, Markl M, Wehrum T, et al. Acute cerebral venous thrombosis: three-dimensional visualization and quantification of hemodynamic alterations using 4-dimensional flow magnetic resonance imaging. Stroke. (2017) 48:671–7. doi: 10.1161/strokeaha.116.015102
- 14. Rivera-Rivera LA, Schubert T, Turski P, Johnson KM, Berman SE, Rowley HA, et al. Changes in intracranial venous blood flow and pulsatility in Alzheimer's disease: a 4D flow MRI study. *J Cereb Blood Flow Metab.* (2017) 37:2149–58. doi: 10.1177/0271678x16661340
- 15. Kim T, Bang JS, Kwon OK, Hwang G, Kim JE, Kang HS, et al. Morphology and related hemodynamics of the internal carotid arteries of moyamoya patients. *Acta Neurochir.* (2015) 157:755–61. doi: 10.1007/s00701-015-2367-y
- 16. Takeuchi S, Karino T. Flow patterns and distributions of fluid velocity and wall shear stress in the human internal carotid and middle cerebral arteries. *World Neurosurg.* (2010) 73:174–85; discussion e27. doi: 10.1016/j.surneu.2009.03.030
- 17. Kim T, Bang JS, Kwon OK, Hwang G, Kim JE, Kang HS, et al. Hemodynamic changes after unilateral revascularization for moyamoya disease: serial assessment by quantitative magnetic resonance angiography. *Neurosurgery*. (2017) 81:111–9. doi: 10.1093/neuros/nyw035

- 18. Research Committee on the Pathology and Treatment of Spontaneous Occlusion of the Circle of Willis, Health Labour Sciences Research Grant for Research on Measures for Infractable Diseases. Guidelines for diagnosis and treatment of moyamoya disease (spontaneous occlusion of the circle of Willis). Neurol Med Chir (Tokyo). (2012) 52:245–66. doi: 10.2176/nmc.52.245
- 19. Schäfer M, Browne LP, Morgan GJ, Barker AJ, Fonseca B, Ivy DD, et al. Reduced proximal aortic compliance and elevated wall shear stress after early repair of tetralogy of Fallot. *J Thorac Cardiovasc Surg.* (2018) 156:2239–49. doi: 10.1016/j.jtcvs.2018.08.081
- 20. Seol HJ, Wang KC, Kim SK, Hwang YS, Kim KJ, Cho BK. Headache in pediatric moyamoya disease: review of 204 consecutive cases. *J Neurosurg.* (2005) 103:439–42. doi: 10.3171/ped.2005.103.5.0439
- 21. Yin H, Liu X, Zhang D, Zhang Y, Wang R, Zhao M, et al. A novel staging system to evaluate cerebral hypoperfusion in patients with moyamoya disease. *Stroke.* (2018) 49:2837–43. doi: 10.1161/strokeaha.118.022628
- 22. Matsushima T, Inoue T, Suzuki SO, Fujii K, Fukui M, Hasuo K. Surgical treatment of moyamoya disease in pediatric patients--comparison between the results of indirect and direct revascularization procedures. *Neurosurgery*. (1992) 31:401–5. doi: 10.1227/00006123-199209000-00003
- 23. Liu ZW, Han C, Wang H, Zhang Q, Li SJ, Bao XY, et al. Clinical characteristics and leptomeningeal collateral status in pediatric and adult patients with ischemic moyamoya disease. *CNS Neurosci Ther.* (2020) 26:14–20. doi: 10.1111/cns.13130
- 24. Kim JM, Lee SH, Roh JK. Changing ischaemic lesion patterns in adult moyamoya disease. *J Neurol Neurosurg Psychiatry*. (2009) 80:36–40. doi: 10.1136/jnnp.2008.145078
- 25. Zhu F, Qian Y, Xu B, Gu Y, Karunanithi K, Zhu W, et al. Quantitative assessment of changes in hemodynamics of the internal carotid artery after bypass surgery for moyamoya disease. *J Neurosurg.* (2018) 129:677–83. doi: 10.3171/2017.5.jns163112
- 26. Gao F, Zhao W, Zheng Y, Li S, Duan Y, Zhu Z, et al. Non-invasive evaluation of cerebral hemodynamic changes after surgery in adult patients with moyamoya using 2D phase-contrast and intravoxel incoherent motion MRI. Front Surg. (2022) 9:773767. doi: 10.3389/fsurg.2022.773767
- 27. Fujimura M, Tominaga T. Current status of revascularization surgery for moyamoya disease: special consideration for its 'internal carotid-external carotid (IC-

- EC) conversion' as the physiological reorganization system. $\it Tohoku~J~Exp~Med.$ (2015) 236:45–53. doi: 10.1620/tjem.236.45
- 28. Shi Z, Ma G, Zhang D. Haemodynamic analysis of adult patients with moyamoya disease: CT perfusion and DSA gradings. *Stroke Vasc Neurol.* (2021) 6:41–7. doi: 10.1136/svn-2019-000317
- 29. Kuwabara Y, Ichiya Y, Otsuka M, Tahara T, Gunasekera R, Hasuo K, et al. Cerebral hemodynamic change in the child and the adult with moyamoya disease. *Stroke.* (1990) 21:272–7. doi: 10.1161/01.str.21.2.272
- 30. Karunanithi K, Han C, Lee CJ, Shi W, Duan L, Qian Y. Identification of a hemodynamic parameter for assessing treatment outcome of EDAS in moyamoya disease. *J Biomech.* (2015) 48:304–9. doi: 10.1016/j.jbiomech.2014.11.029
- 31. Wang M, Yang Y, Zhang W, Zhou F, Zhang X, Zhang J, et al. Risk factors for cerebrovascular events in moyamoya angiopathy using 4D flow MRI: a pilot study. *J Magn Reson Imaging.* (2023) 58:61-8. doi: 10.1002/jmri.28522
- 32. Kim YJ, Lee DH, Kwon JY, Kang DW, Suh DC, Kim JS, et al. High resolution MRI difference between moyamoya disease and intracranial atherosclerosis. *Eur J Neurol.* (2013) 20:1311–8. doi: 10.1111/ene.12202
- 33. Takagi Y, Kikuta K, Nozaki K, Hashimoto N. Histological features of middle cerebral arteries from patients treated for moyamoya disease. *Neurol Med Chir (Tokyo)*. (2007) 47:1–4. doi: 10.2176/nmc.47.1
- 34. Kwak BR, Bäck M, Bochaton-Piallat ML, Caligiuri G, Daemen MJ, Davies PF, et al. Biomechanical factors in atherosclerosis: mechanisms and clinical implications. *Eur Heart J.* (2014) 35:3013–20, 20a-20d. doi: 10.1093/eurheartj/ehu353
- $35.\,Xiao\,H, Lu\,M, Lin\,TY, Chen\,Z, Chen\,G, Wang\,WC, et al.$ Sterol regulatory element binding protein 2 activation of NLRP3 inflammasome in endothelium mediates hemodynamic-induced atherosclerosis susceptibility. Circulation. (2013) 128:632–42. doi: 10.1161/circulationaha.113.002714
- 36. Cuhlmann S, Van der Heiden K, Saliba D, Tremoleda JL, Khalil M, Zakkar M, et al. Disturbed blood flow induces RelA expression via c-Jun N-terminal kinase 1: a novel mode of NF- κ B regulation that promotes arterial inflammation. *Circ Res.* (2011) 108:950–9. doi: 10.1161/circresaha.110.233841
- 37. Schnell S, Wu C, Ansari SA. Four-dimensional MRI flow examinations in cerebral and extracerebral vessels ready for clinical routine? *Curr Opin Neurol.* (2016) 29:419–28. doi: 10.1097/wco.000000000000341